Received: 25 May 2021 | Revised: 26 January 2022 | Accepted: 31 January 2022

DOI: 10.1111/mec.16386

ORIGINAL ARTICLE

MOLECULAR ECOLOGY WILEY

Temporal changes in pathogen diversity in a perennial plant–pathogen–hyperparasite system

Lea Stauber[1,2,3] | Daniel Croll[2] | Simone Prospero[1]

[1]Swiss Federal Institute for Forest, Snow and Landscape Research (WSL), Birmensdorf, Switzerland

[2]Laboratory of Evolutionary Genetics, Institute of Biology, University of Neuchâtel, Neuchâtel, Switzerland

[3]Department of Environmental Sciences, University of Basel, Basel, Switzerland

Correspondence
Simone Prospero, Swiss Federal Institute for Forest, Snow and Landscape Research (WSL), Birmensdorf, Switzerland.
Email: simone.prospero@wsl.ch

Funding information
Schweizerischer Nationalfonds zur Förderung der Wissenschaftlichen Forschung, Grant/Award Number: 170188

Handling Editor: Sara Branco

Abstract

Hyperparasites can affect the evolution of pathosystems by influencing the stability of both pathogen and host populations. However, how pathogens of perennial hosts evolve in the presence of a hyperparasite has rarely been studied. Here, we investigated temporal changes in genetic diversity of the invasive chestnut blight pathogen *Cryphonectria parasitica* in the presence of its parasitic mycovirus *Cryphonectria hypovirus 1* (CHV1). The virus reduces fungal virulence and represents an effective natural biocontrol agent against chestnut blight in Europe. We analysed genome-wide diversity and CHV1 prevalence in *C. parasitica* populations in southern Switzerland that were sampled twice at an interval of about 30 years. Overall, we found that both pathogen population structure and CHV1 prevalence were retained over time. The results suggest that recent bottlenecks have influenced the structure of *C. parasitica* populations in southern Switzerland. Strong balancing selection signals were found at a single vegetative incompatibility (*vic*) locus, consistent with negative frequency-dependent selection imposed by the vegetative incompatibility system. High levels of mating among related individuals (i.e., inbreeding) and genetic drift are probably at the origin of imbalanced allele ratios at *vic* loci and subsequently low *vc* type diversity. Virus infection rates were stable at ~30% over the study period and we found no significant impact of the virus on fungal population diversity. Consequently, the efficacy of CHV1-mediated biocontrol was probably retained.

KEYWORDS
biological control, biological invasion, evolutionary dynamics, vegetative incompatibility

1 | INTRODUCTION

Host–pathogen interactions drive the evolution of pathosystems by determining disease dynamics through selection on pathogen virulence and host resistance. The evolution of pathosystems may additionally be shaped by hyperparasites, which infect the pathogens themselves, thereby influencing disease dynamics (Parratt & Laine, 2016). Pathogen–hyperparasite interactions may underlie similar evolutionary forces as the primary host–pathogen interactions. For instance, temporal changes in genome structure were found in bacteriophages attacking gut bacteria, suggesting antagonistic co-evolution (Reyes et al., 2013). Moreover, experimental evidence for co-evolutionary dynamics was detected between bacterial populations on horse chestnut trees (*Aesculus hippocastanum*)

and hyperparasitic phages (Koskella, 2013). Thus, hyperparasites likely represent a major selective force in the evolution of their pathogenic host, impacting evolutionary rates and genetic turnover within pathogen populations (Ford et al., 2017). The effect of hyperparasites may be even more pronounced in perennial pathosystems, in which pathogen generation times are much shorter compared to their host generation times. Shorter generation times make pathogen populations less subjected to extinction dynamics. On the other hand, long-living hosts (e.g., trees) are prone to extended inoculum build up, while selection for resistance is slow (Barrett et al., 2008; Dumartinet et al., 2020; Hessenauer et al., 2021; Tellier & Brown, 2009). From a tree host perspective, hyperparasites that significantly reduce the fitness of their pathogenic host are beneficial as they increase the chances of survival. Hence, such hyperparasites represent promising agents for biocontrol of pathogens in agricultural and forest systems (Branine et al., 2019; Mei et al., 2020; Tian et al., 2007). However, the impact of hyperparasites on shaping pathogen populations in perennial systems and the potential consequences for long-term success of biocontrol have rarely been studied.

In forests, one of the most well-known examples for a successful biocontrol agent is the hyperparasite *Cryphonectria hypovirus 1* (CHV1), which induces hypovirulence in the chestnut blight fungus *Cryphonectria parasitica* (Murr). Barr. (Van Alfen, 1982; Elliston, 1982; Grente, 1965). CHV1, which belongs to the family Hypoviridae, is a positive-strand RNA virus located in the cytoplasm of *C. parasitica* (Choi & Nuss, 1992). The virus significantly reduces virulence, growth and sporulation of the infected fungal strain, subsequently leading to recovery of infected chestnut trees (Anagnostakis, 1982; Brusini et al., 2017; Rigling & Prospero, 2018). On a molecular level, CHV1 has been found to significantly alter expression of genes in *C. parasitica* associated with virulence, primary and secondary metabolism, as well as carbohydrate metabolization (Chun et al., 2020). The virus has been used over decades as a naturally occurring or artificially released biocontrol agent against chestnut blight in Europe (e.g., Diamandis et al., 2014; Heiniger & Rigling, 2009). Yet, the long-term presence of CHV1 in European *C. parasitica* populations raises important questions on the virus' effects on the temporal dynamics of *C. parasitica* diversity and selection pressures.

C. parasitica, the fungal host of CHV1, has emerged as an invasive pathogen in North America and Europe, causing lethal bark lesions (so called cankers) on non-Asian chestnut species (*Castanea* spp.) (Rigling & Prospero, 2018). During the colonization process of North America and Europe, *C. parasitica* underwent multiple genetic bottlenecks that strongly shaped its population structure and diversity in the invasive range (Dutech et al., 2012). Accordingly, European *C. parasitica* populations are characterized by lower genetic diversity compared to native Asian, but also to invasive North American populations (Dutech et al., 2012; Milgroom & Cortesi, 1999). The low genetic diversity of European *C. parasitica* populations has partially been attributed to higher rates of clonality, facilitating colonization of new areas in the absence of mating partners (Demené et al., 2019; Milgroom et al., 1996; Sotirovski et al., 2004; Stauber et al., 2021). For instance, southeastern Europe was predominantly colonized by a single clonal *C. parasitica* lineage, which probably emerged from a sexually reproducing European bridgehead population (Stauber et al., 2021). Sexual reproduction has predominantly been observed in long established and genetically more diverse European *C. parasitica* populations, including those in southern Switzerland, northern Italy and Croatia (Ježić et al., 2018; Prospero & Rigling, 2012; Stauber et al., 2021). Sexual reproduction in *C. parasitica* is controlled by a single mating (*MAT*) locus with two alleles (*MAT-1* or *MAT-2*) (McGuire et al., 2001). For successful mating, opposite mating types from two individuals are required, but fertile individuals carrying both mating type alleles (so called heterokaryons) are occasionally observed (McGuire et al., 2004). Sexual recombination is considered to be a major driver of population diversification, including diversification at the loci that control hypovirus transmission between fungal strains.

As CHV1 has no extracellular phase, it can only be transmitted horizontally via hyphal anastomosis between fungal individuals, or vertically through asexual spores (conidia) (Rigling & Prospero, 2018). In contrast, sexual spores (ascospores) have consistently been found to be virus-free (Anagnostakis, 1988; Prospero et al., 2006), even though virus-infected conidia can act as male partners (spermatia) in sexual crosses (Anagnostakis, 1988). The virus induces female sterility, thereby preventing fungal sexual reproduction among virus-infected fungal host strains (Nuss, 2005). Horizontal CHV1 transmission is regulated by at least six unlinked biallelic *vic* loci (Cortesi & Milgroom, 1998). Successful CHV1 transmission occurs when fungal individuals share the same alleles at all *vic* loci (i.e., belong to the same vegetative compatibility ([*vc*] type), whereas allelic polymorphism at the *vic* loci strongly reduces transmission rates (Cortesi et al., 2001). Sexual recombination between individuals of different *vc* types can generate new allelic combinations at *vic* loci, driving *vc* type diversification within fungal populations and limiting CHV1 spread. However, incompatibility barriers may only partially and asymmetrically affect CHV1 transmission, depending on which *vic* loci are polymorphic and on the identity of the virus donor strain (Cortesi et al., 2001). Hence, maintaining balanced and high *vic* allele diversity, as well as selection at *vic* loci involved in asymmetric virus transmission are probably important evolutionary forces to reduce prevalence of the hyperparasite within fungal host populations (Milgroom et al., 2018). In Europe, *vc* type diversity in *C. parasitica* populations is lower than expected under random mating, which facilitates the natural spread of CHV1 (Krstin et al., 2011; Prospero & Rigling, 2012). Concurrently, spatial and temporal variation of CHV1 prevalence has been observed, suggesting fluctuating dynamics between CHV1 and its fungal host (Bryner et al., 2014; Ježić et al., 2018). However, how these dynamics shape the evolution of European *C. parasitica* populations and why sexual recombination has not resulted in significantly higher *vc* type diversity reducing CHV1 spread in Europe remain largely unknown.

In this study, we analysed the genetic diversity in European *C. parasitica* populations with natural CHV1 occurrence. For this, we sampled three *C. parasitica* populations in the canton Ticino (southern Switzerland) at two time points over three decades. In this region,

European chestnut is the dominant tree species, forming a largely continuous forest belt which ranges up to 900 m above sea level. Chestnut blight was first officially reported in 1948, probably after spontaneous spread from neighbouring northern Italy (Heiniger & Rigling, 1994). CHV1-infected chestnut blight cankers were first observed in 1975 and natural hypovirulence is currently widespread. *C. parasitica* populations in southern Switzerland are considered to be sexually reproducing, as both mating types are present and sexual fruiting bodies are frequently observed in the field (Bissegger et al., 1997; Prospero et al., 2006). With this study design, we (i) analysed differentiation of the pathogen populations across the two time points, (ii) estimated the contribution of sexual and asexual reproduction to the observed diversity, and (iii) tested for signatures of recent positive and balancing selection in gene functions encoded across the genome. For our analyses, we sequenced whole genomes of 142 *C. parasitica* isolates, which were obtained from three populations sampled twice in the 1990s and in 2019.

2 | METHODS

2.1 | Origin of *Cryphonectria parasitica* isolates

The 142 *C. parasitica* isolates analysed in this study originated from three sampling sites (Gnosca, Lumino and Novaggio) located in the canton Ticino in southern Switzerland, at a distance ranging from 3.7 to 30 km (Figure 1). Each site was considered to represent a different *C. parasitica* population. About half of the isolates (n = 74) were obtained from the WSL fungal collection, representing the first sampling in 1990 (Lumino and Gnosca; Bissegger et al., 1997; Prospero & Rigling, 2012) and in 1996 (Novaggio; Prospero & Rigling, 2012) (Tables 1 and S1). An additional 68 isolates originated from resampling of the three populations in 2019 (Tables 1 and S1). These isolates were recovered from randomly selected bark cankers, as described in Prospero and Rigling (2012). The cankers sampled in 2019 likely did not correspond to those of the first sampling in the 1990s. For all isolates, mating and *vc* types were determined following the protocol of Cornejo et al. (2019). Ambiguous molecular *vc* type results were additionally confirmed by pairing tester strains of known *vc* type with the unknown isolate and assessing the merging/barrage response (Bissegger et al., 1997). Isolates were prepared for whole-genome sequencing as described in Stauber et al. (2021). Sequencing was performed on the NovaSeq6000 platform (Illumina) at the Functional Genomics Center Zurich (FGCZ). To investigate the population genetic structure of the Ticino populations in a broader context, we additionally included 95 sequenced isolates from Stauber et al. (2020) and Stauber et al. (2021), covering the European and North American *C. parasitica* diversity (Table S1). All sequences were trimmed and aligned to the *C. parasitica* reference genome EP155 (Crouch et al., 2020), and variants were called and filtered as described in Stauber et al. (2021). For removal of single nucleotide prolmorphsisms (SNPs) associated with the mating type region, we identified highly associated SNPs in an association study with TASSEL 5 (Bradbury et al., 2007; Stauber et al., 2021). We subsequently removed all SNPs in the mating type region with a p-value threshold of $p \leq 1\times10^{-5}$ (Figure S1).

2.2 | CHV1 prevalence in Ticino populations

To assess CHV1 presence in *C. parasitica* isolates from Gnosca, Lumino and Novaggio, we performed a rapid one-step reverse transcriptase polymerase chain reaction (RT-PCR) (Urayama et al., 2015). For this, isolates were cultured on potato dextrose agar (PDA, 39 g L^{-1}; BD Becton, Dickinson and Company) and incubated for 5 days at room temperature and natural daylight. Hyphae of growing cultures were then transferred into PCR plate wells, by vertically piercing through the culture with a sterile toothpick and smearing the adhered residues into the PCR plate wells. Then, 7 µl of reaction mix from the PrimeScript One Step RT-PCR kit version 2 (Takara Bio) was added to each well on ice together with the CHV1 forward and reverse primers hvep1 and hvep2 (Gobbin et al., 2003). The RT-PCR was run following an adjusted protocol of Urayama et al. (2015), with 50°C for 30 min for reverse transcription, followed by 94°C for 2 min for DNA polymerase activation, then 33 cycles of denaturation at 94°C for 30 s, annealing at 58°C for 30 s and extension at 72°C for 1 min. Virus presence was then confirmed through gel electrophoresis (1.2% agarose gel, 50 min, 90 V DC) with bands at 350 bp.

2.3 | Analysis of population structure

For analysis of the European and North American population structure we performed a discriminant analysis of principal components (DAPC) as implemented in the R package adegenet version 2.1.4 (Jombart, 2008; Jombart et al., 2010). To estimate the optimum number of retained PCs, cross-validation was performed using the xvalDapc function from the adegenet package (Jombart, 2008; Jombart et al., 2010). Furthermore, DAPC was used to investigate the population structure within the Ticino populations across sampling points. Additionally, we investigated the Ticino diversity by performing a principal component analysis (PCA) as implemented in the R package ade4 version 1.7.15 (Bougeard & Dray, 2018). Moreover, we generated unrooted phylogenetic networks with SPLITSTREE version 4.14.6 (Huson et al., 2008). To test for temporal differentiation between the populations of the 1990s and 2019 samplings, we performed an analysis of molecular variance (AMOVA), using the R package poppr version 2.9.3 (Kamvar et al., 2014). The significance of temporal differentiation was tested by using the randtest() function from the ade4 package with *nrepet* = 999.

2.4 | Population genetic and relatedness analyses

We calculated nucleotide diversity for European isolates, as well as both Ticino samplings (1990s and 2019) separately with VCFTOOLS

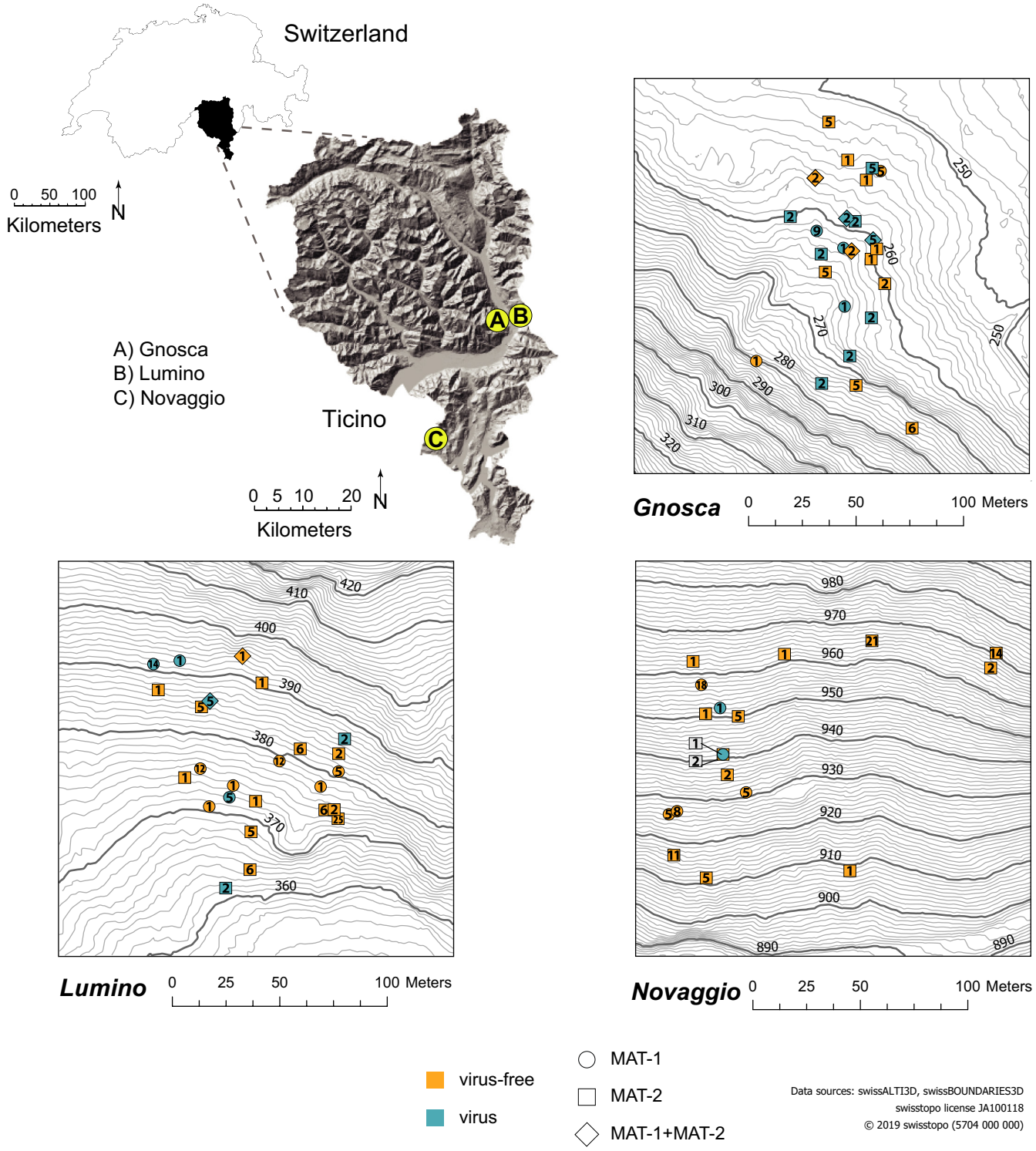

FIGURE 1 Geographical map showing the *Cryphonectria parasitica* populations which were sampled in the 1990s and 2019 in Ticino (southern Switzerland). Top right and bottom panels show the geographical locations of sampled trees in 2019 at all three sampling sites (Gnosca, Lumino and Novaggio). Information on virus infection (blue = virus-infected, orange = virus-free), *vc* types (numbers) and mating types (circle = *MAT-1*, square = *MAT-2*, diamond = heterokaryon) of cankers sampled in 2019 is given

version 0.1.15 (Danecek et al., 2011). We used the same tool to calculate allele frequencies in each of the Ticino samplings. To investigate pairwise identity among individuals of the same sampling, we conducted an identity-by-state (IBS) analysis as implemented in the R package SNPrelate version 1.22.0 (Zheng et al., 2012). To further investigate relatedness of individuals within the 1990s and 2019 samplings, we performed a pairwise identity-by-descent (IBD) analysis for haploid organisms using a hidden Markov model, as implemented in the HMMIBD software (Schaffner et al., 2018). For this, we changed the number of analysed scaffolds to *nchrom* = 13. Moreover, the default recombination rate (*r*) was changed to estimates for *C. parasitica* with $r = \rho/2^{*}N_e$. The mean effective population size ($2^{*}N_e$) and the mean

TABLE 1 Geographical origin and sampling year of the 142 *Cryphonectria parasitica* isolates from Ticino (southern Switzerland) analysed in this study

Population	Coordinates[a]	Sampling year	Samples (*n*)	Reference
Lumino	46.236031N, 9.069902E	1990	24	Bissegger et al. (1997)
		2019	25	This study
Gnosca	46.228774N, 9.022628E	1990	25	Prospero and Rigling (2012)
		2019	25	This study
Novaggio	46.023190N, 8.834188E	1996	25	Prospero and Rigling (2012)
		2019	18	This study

[a]For the geographical location, see Figure 1.

TABLE 2 Diversity statistics showing the number of samples, number of SNPs, per cent singletons, SNP density range and nucleotide diversity (π) for the broader USA and European *Cryphonectria parasitica* populations, as well as populations from Ticino (southern Switzerland) in the 1990s and in 2019

Population	Samples (*n*)	SNPs (*n*)	Singletons (%)	SNP density	π
USA and Europe	95	8,360	24	0–80 kb^{-1}	9.58×10^{-6}
Ticino 1990s	74	3,721	13.20	0–29 kb^{-1}	2.75×10^{-6}
Ticino 2019	68	6,724	40	0–53 kb^{-1}	2.47×10^{-6}

population recombination rate (ρ) were inferred with LDHAT (McVean & Auton, 2007; Stauber et al., 2021). We additionally annotated synonymous and nonsynonymous mutations with SNPEFF version 5.0 (Cingolani et al., 2012). To assess the relative importance of *vc* types, mating types, sampling location and CHV1 presence/absence on the observed genetic diversity as inferred by IBS in each sampling, we ran a permutational multivariate analysis of variance (PERMANOVA; Anderson, 2001) using the R package vegan version 2.5.6 (Oksanen et al., 2019). The potential number of *vc* types in each population at both samplings under random mating was calculated using the formula 2^n, where n = number of polymorphic *vic* loci at the specific sampling. Differences in *vc* type diversity between the two samplings were tested for significance by performing a chi-square test. We additionally tested if allele frequencies of individual *vic* loci significantly deviated from 0.5 by performing an exact binomial test.

2.5 | Selection analyses

We performed genome-wide scans for positive selection by implementing the pipeline and parameters described in Stauber et al. (2021). Briefly, we used RAISD version 2.9 (Alachiotis & Pavlidis, 2018) on both the 1990s and 2019 sampling data sets. To account for false positive signals due to demographic history of the populations, we performed simulations under bottleneck, neutral and expansion scenarios, using the software MS (Hudson, 2002). Functional annotation of proteins predicted to be under positive selection was done with INTERPROSCAN version 5.31–70.0 (Jones et al., 2014). We performed genome-wide scans for signals of balancing selection in the 1990s and 2019 sampling sets, as well as for the simulated data sets (i.e., bottleneck, neutral and expansion simulations) using the software BETASCAN (Siewert & Voight, 2017), with the parameters -m 0.1 -theta 558 -p 20. Values for the -theta parameter were derived from Stauber et al. (2021). Furthermore, we calculated Tajima's *D* in 5-kb windows using VCFTOOLS. To identify whether regions under selection were overlapping with known *vic* loci, we performed a genome-wide association study (GWAS) using TASSEL version 5 (Bradbury et al., 2007). We identified SNPs associated with known *vic* loci and inferred their chromosomal locations (Table S2). As *vic3* was found to be monomorphic in our data set, we identified the chromosomal locations of the *vic3* locus by searching the publicly available *vic3a* (GenBank accession HG799044.1; Zhang et al., 2014) against the *C. parasitica* reference genome using BLAST.

2.6 | Spatial structure of Ticino populations

For spatial visualization of *C. parasitica* genotypes as well as CHV1 distribution at the three sampling sites, GPS coordinates were collected with the app My GPS Location for each sampled tree in 2019 (second sampling; Table S1). Topographic maps were generated in ARCGIS PRO version 2.3.0 (ESRI Inc.), using the swissALTI3D elevation model and the swissBOUNDARIES3D for all administrative units and national boundaries (swisstopo licence: JA100118).

3 | RESULTS

3.1 | Population structure in southern Switzerland and across Europe

Since *Cryphonectria parasitica* populations in central Europe were probably established by North American (USA) sources alone (Dutech et al., 2012; Stauber et al., 2021), we explored the diversity and structure of the three *C. parasitica* populations in Ticino (Figure 1) in a broader context. For this, we included samples of

other European and of North American origin. We found the highest number of SNPs ($n = 8360$) in the broader US/European populations, followed by the Ticino 2019 populations ($n = 6724$) and the Ticino 1990s populations ($n = 3721$; Table 2). Of note, 40% of all SNPs in the Ticino 2019 data set were found to be singletons. We also investigated the SNP density across the genome. While SNP density was low for the majority of the 1-kb windows, we detected several clusters with high SNP density in multiple chromosomal regions (Figure S2). Most of these clusters were shared among the USA/Europe, Ticino 1990s and Ticino 2019 sample sets (Figure S2). Overall, SNP density ranged from 0 to 80 SNPs kb^{-1} in the USA and European sample sets, as well as from 0–29 SNPs kb^{-1} and 0 to 53 SNPs kb^{-1} for the Ticino 1990s and Ticino 2019 sample sets, respectively (Figure S2; Table 2). Nucleotide diversity within European and USA samples was $\pi = 9.58 \times 10^{-6}$ compared to the Ticino populations of the 1990s and 2019 with $\pi = 2.75 \times 10^{-6}$ and $\pi = 2.47 \times 10^{-6}$, respectively (Table 2). The DAPC including all samples from Ticino (1990s and 2019), as well as other European and USA samples revealed no distinct clustering of populations, confirming the overlap in genotypes from the USA, central Europe and Ticino (Figure 2a; Stauber et al., 2021).

3.2 | Temporal changes in population structure in Ticino

We investigated temporal changes in population structure of *C. parasitica* in Ticino through DAPC, PCA and phylogenetic network analyses. Overall, we detected no substantial changes in population structure over the period of ~30 years between the two samplings (Figure 2b–d). While in the DAPC the Lumino 2019 population appeared to be slightly segregated from the other populations (Figure 2b), a subsequent analysis of temporal and spatial population differentiation using AMOVA revealed no statistically significant differentiation (clone corrected: $\Phi \leq -0.002$, $p > .05$; Table S2). In both samplings we found genetically closely related, as well as distant genotypes. The closely related genotypes were predominantly of *vc* types EU-01, EU-02, EU-05 and EU-06. These genotypes showed clustering in both the 1990s and the 2019 samplings, but appeared to be slightly more aggregated in the 2019 sampling (Figure 2c). Moreover, the phylogenetic networks of the 1990s and 2019 data sets showed clear reticulations, indicating recombination (pairwise homoplasy index [PHI]: $p < .001$, Figure 2c). The most distant genotypes were of *vc* type EU-09 for both time points (Figure 2c). Notably, the EU-09 isolate (GNO32) found in 2019 in Gnosca was a clone of the EU-09 isolate (M1243) recovered in 1990 in Lumino (Figure 2d).

3.3 | Genotypic similarity and relatedness

We analysed allele frequencies to gain insight into the genetic structure of the fungal populations across sampling time points. Compared to the 1990s sampling, the 2019 sampling showed an increase of rare alleles and a higher abundance of (nearly) fixed alleles (Figure 3a). The number of deleterious mutations remained at low levels in both the 1990s and 2019 samplings, suggesting removal of deleterious mutations through recombination (Figure 3b). To quantify genetic relatedness among genotypes within the 1990s and 2019 samplings, we analysed pairwise IBS and IBD between individuals. Individuals were found to be highly genetically similar within the 1990s and 2019 samplings, with a mean IBS of 0.92 (SD = 0.06) in the 1990s sampling and a mean IBS of 0.94 (SD = 0.06) in the 2019 sampling. Genetic similarity increased significantly in 2019 (*t* test mean difference $p < .001$), with 70.2% of isolate pairs showing IBS values ≥0.95, compared to 31.9% in the 1990s (Figures 3c and S3). We additionally analysed pairwise IBD with HMMIBD (Schaffner et al., 2018), using an estimated recombination rate of $r = 1.97 \times 10^{-4}$ for *C. parasitica*. In accordance with IBS, IBD values increased significantly in the 2019 sampling (*t* test mean difference $p < .001$), with mean IBD = 0.62 (SD = 0.24) for the 1990s sampling and mean IBD = 0.71 (SD = 0.24) for the 2019 sampling, respectively (Figures 3c and S3). Only a small fraction of isolate pairs (1990s sampling: 0.96%, $n = 26$; 2019 sampling: 0.92%, $n = 21$) appeared to be clonemates (IBD = 1, Figure 3c), suggesting that high genetic similarity in *C. parasitica* populations in Ticino is largely explained by mating among closely related individuals rather than clonal reproduction.

3.4 | Detection of genome-wide signals of positive and balancing selection

We investigated genome-wide signatures of positive selection for the 1990s and 2019 samplings using RAISD (Alachiotis & Pavlidis, 2018). To control for potential demographic effects on selection signals, we additionally ran selection scans on simulated data sets to determine thresholds above which selection signals are most likely to be exceeding demographic effects. Stauber et al. (2021) previously attempted to reconstruct the demographic history of central European *C. parasitica* populations. However, due to an irregular folded site frequency spectrum (SFS), parameter optimization was not reached and no particular demographic model could be fitted to the central European *C. parasitica* populations. The folded SFS in the present Ticino 1990s and 2019 sample sets were irregular (Figure S4). Hence, we decided to account for demographic history by simulating populations under bottleneck, neutral and expansion models. The strongest selection signal in the 1990s data set was found on scaffold 4 ($\mu = 72.24$), encompassing an ~330-kb region (Figure 4a). The second strongest peak ($\mu = 52.51$) spanning an ~735-kb region was on scaffold 5. This region is overlapping with the *vic3* locus and an adjacent predicted heterokaryon incompatibility protein (*HET*), with a putative function in fungal nonself recognition (Glass & Kaneko, 2003). Notably, recent transcriptomic analyses found significant upregulation of this *HET* gene (referred to as *dev3-2*, gene ID: 262887) upon an incompatibility reaction triggered by alleles at the locus *vic3* (Belov et al., 2021, Figure 4a). The third strongest outlier

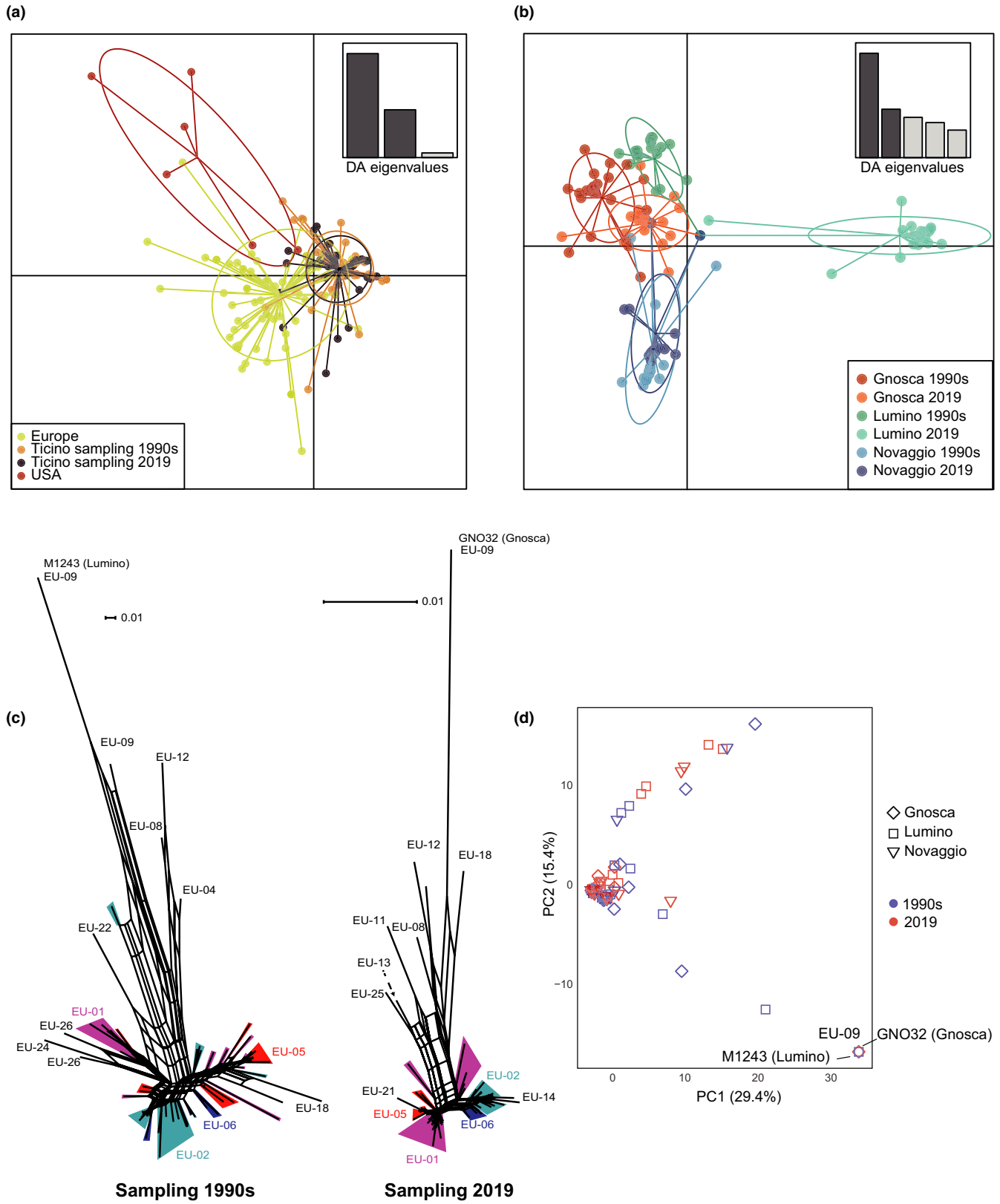

FIGURE 2 Genetic diversity and phylogenetic reconstruction of *Cryphonectria parasitica* populations. (a) Discriminant analysis (DAPC) of populations in Ticino and the broader European and North American diversity. (b) DAPC of the populations in Ticino from both samplings (1990s and 2019). (c) SPLITSTREE phylogenetic network comparison of Ticino populations from the first (left) and second (right) sampling. Scale bars indicate genetic distances. Dominant *vc* types are highlighted in colours. (d) PCA of Ticino population structure. Colours mark samplings (blue = first sampling, red = second sampling), and shapes indicate sampling locations (i.e., Gnosca, Lumino, Novaggio)

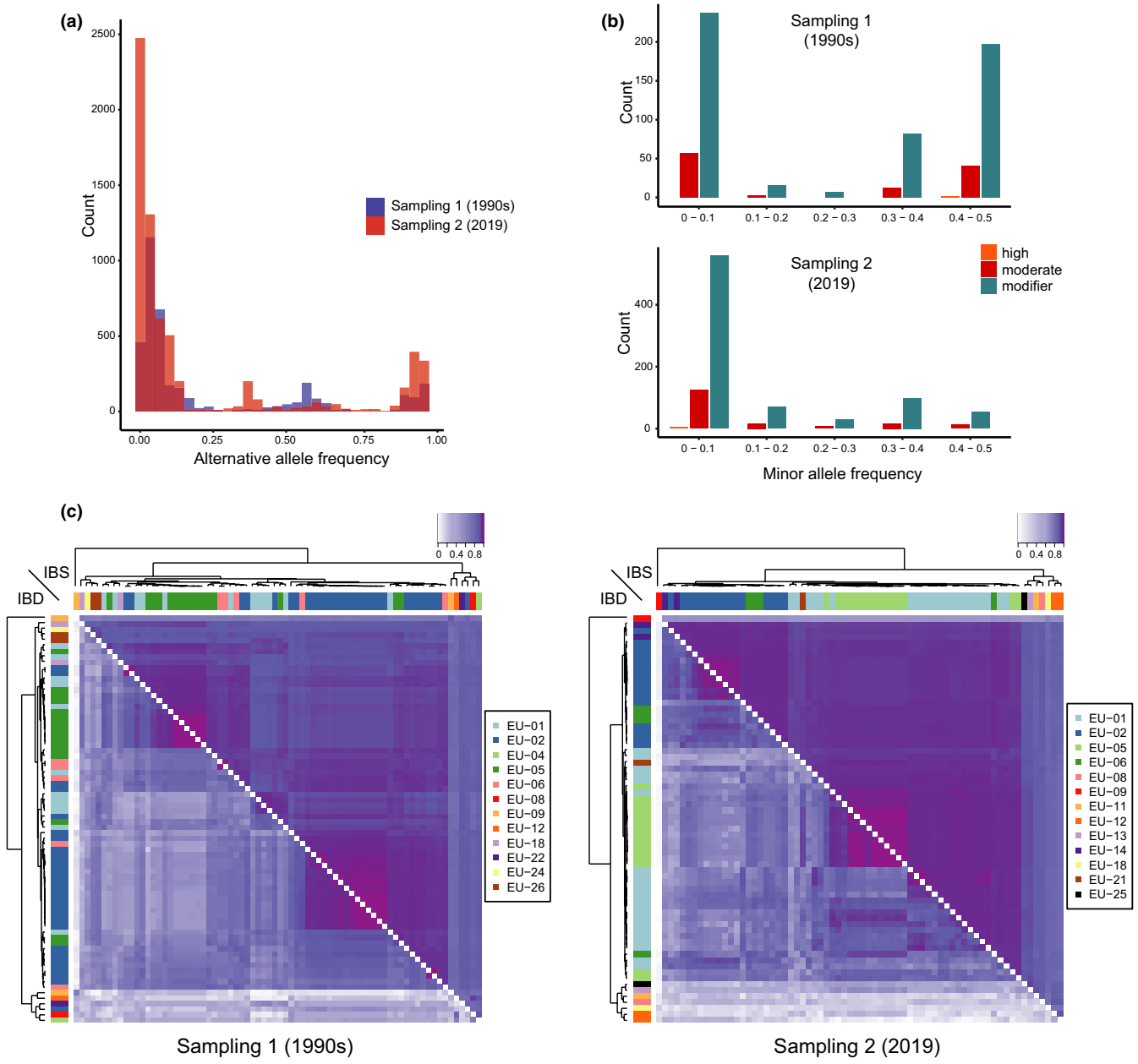

FIGURE 3 Polymorphism spectra, identity by state (IBS) and identity by descent (IBD) of *Cryphonectria parasitica* isolates in Ticino (southern Switzerland). (a) Alternative allele frequencies of the first (blue) and second (red) Ticino sampling. (b) Minor allele frequency spectra of high, moderate and modifier impact mutations in both Ticino samplings. (c) Heatmaps of pairwise IBS and IBD in the first (left) and second (right) Ticino sampling. Upper heatmap panels show pairwise IBS and lower panels give pairwise fraction of site IBD between isolates. Dendrograms show IBS similarity among isolates. Coloured bars indicate *vc* types of individual isolates

was found on scaffold 6, spanning an ~415-kb region. Within the positively selected region on scaffold 6 we detected a gene involved in pigment formation (gene ID: 263100), which was also found to be highly upregulated upon vegetative incompatibility formation (Belov et al., 2021; Table S3). In the 2019 sample sets we found numerous regions under positive selection which were above the demographic thresholds (Figure 4a). The higher number of loci with selection signatures may originate from strong recent selection or from high

FIGURE 4 Genome-wide scans for signatures of selection in the 1990s and 2019 samplings. (a) Screens for positive selection with RAISD. Demographic history effects were accounted for through simulations under neutral, expansion and bottleneck scenarios. The dashed lines show the maximum values observed in the simulated data sets of the corresponding demographic models. Labelled points indicate regions in which known *vic* loci or putative heterokaryon incompatibility genes were found. (b) Scans for balancing selection using BETASCAN. (c) Values for Tajima's *D* calculated in 5-kb windows across the genome

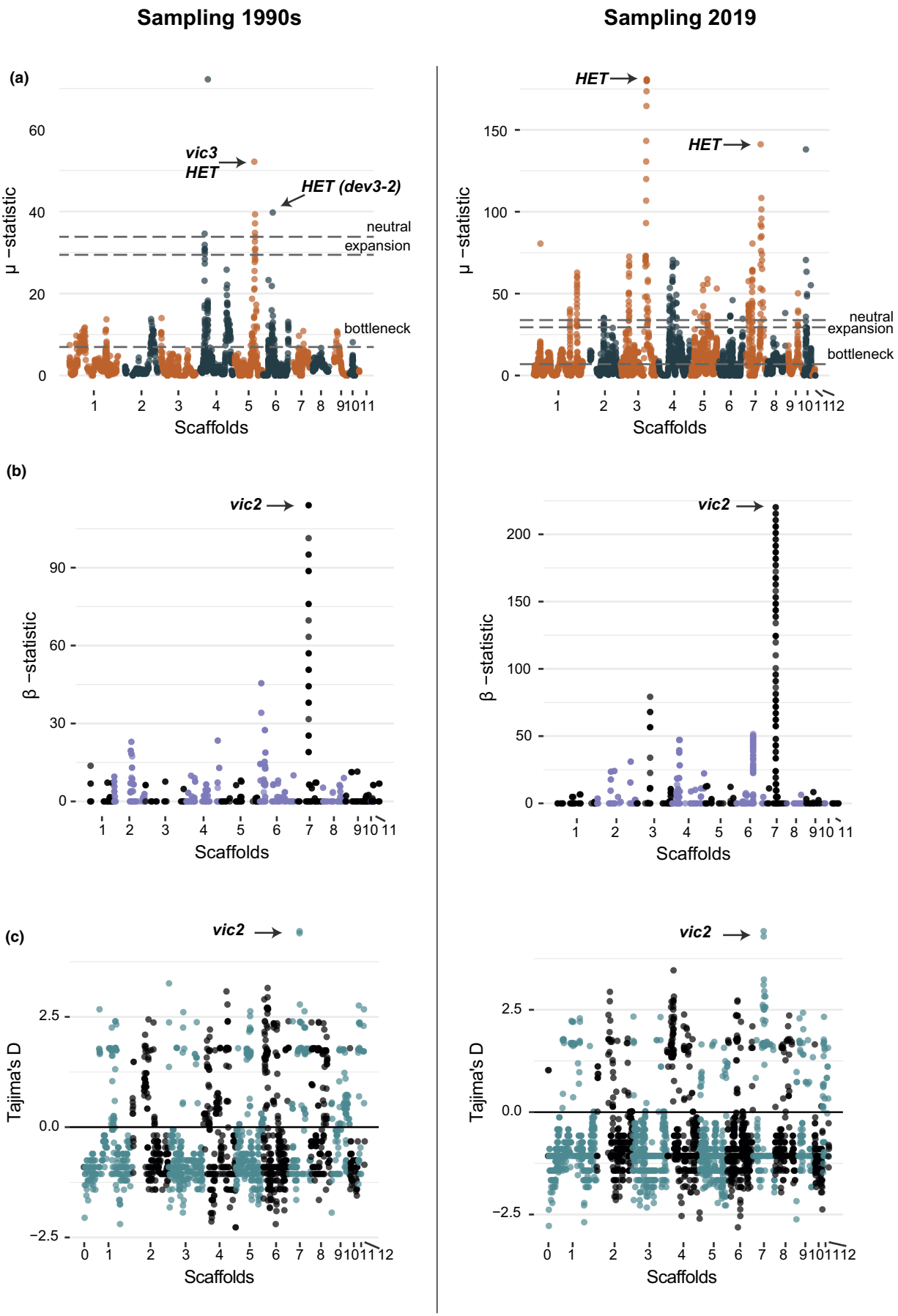

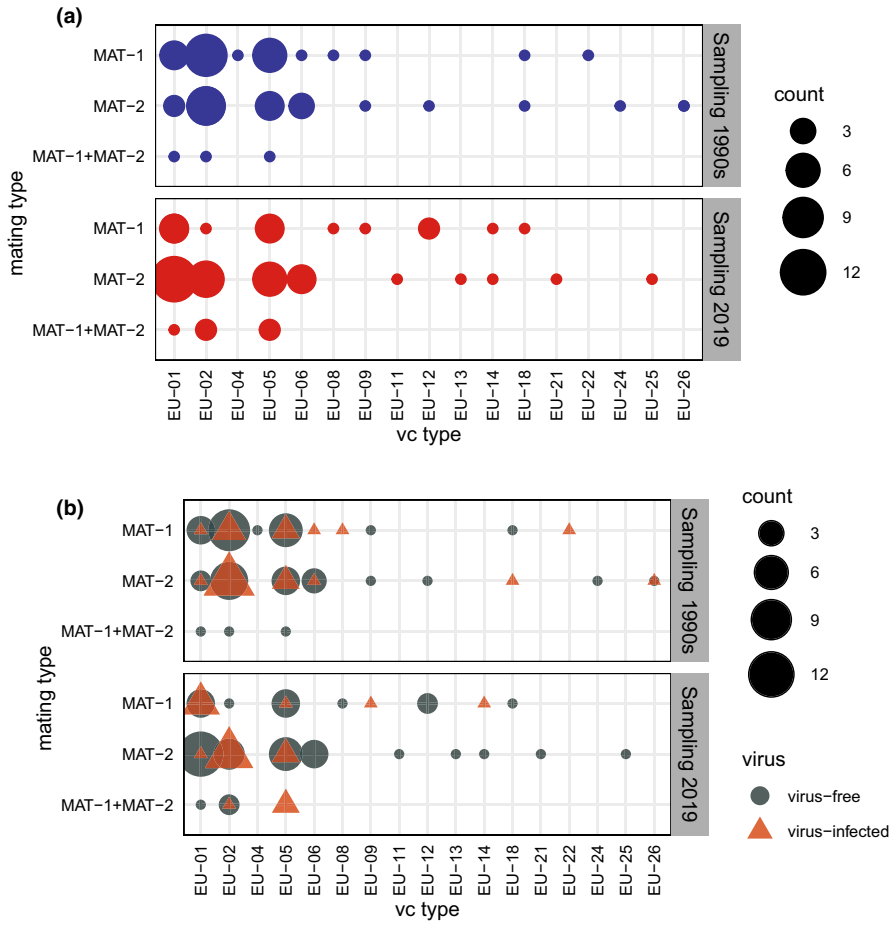

FIGURE 5 Mating type and vegetative compatibility (*vc*) type ratios and virus incidence of *Cryphonectria parasitica* genotypes from Ticino (southern Switzerland). (a) Mating type counts among *vc* types. (b) Count of virus-free (blue circles) and virus-infected isolates across mating types and *vc* types

levels of highly genetically similar or near-clonal isolates emerging through inbreeding or selfing. The two most striking outliers were found on scaffold 3 (μ = 180.9; ~1055-kb region) and on scaffold 7 (μ = 141.2; ~1385-kb region). The region on scaffold 3 is overlapping with two genes encoding *HET* domains, while the region on scaffold 7 overlaps with three *HET* genes (Figure 4a). Whether these *HET* genes are involved in the formation of incompatibility barriers and can potentially inhibit mycovirus transmission in *C. parasitica* remains to be investigated. A detailed list of chromosomal regions with signatures of positive selection is provided in Table S3. Functional annotations (PFAM) of proteins encoded by genes in regions with positive selection signatures are provided in Tables S4 and S5.

We additionally performed genome-wide scans for signals of balancing selection for the 1990s and 2019 samplings and found a strong peak on scaffold 7 in both samplings (Figure 4b, sampling 1990s: β_{max} = 114.02; sampling 2019: β_{max} = 220.16). The peak overlaps with the vegetative incompatibility locus *vic2*, suggesting that this locus might be under balancing selection. The genomic position of the *vic2* locus was identified through GWAS, which revealed significantly associated SNPs at all five polymorphic *vic* loci, including *vic2* ($p \leq 9.82 \times 10^{-55}$). However, balancing selection scans for the simulated data were inconclusive and we were unable to determine a threshold for signatures of balancing selection probably exceeding demographic effects. We additionally calculated Tajima's *D* in a 5-kb window across the genome and found a single positive outlier value on scaffold 7 in the 1990s (*D* = 4.44) and 2019 (*D* = 4.41) sample sets (Figure 4c). The outlier again overlapped with the *vic2* locus, matching the findings of the BETASCAN analysis. Moreover, the *vic2* locus was found to be the only analysed *vic* locus where allele frequencies did not significantly deviate from 0.5 in both samplings (exact binomial test $p > .05$).

3.5 | Mating type and vegetative compatibility diversity

Given the observed population structure and the frequent observation of perithecia in the field (Bissegger et al., 1997; Prospero et al., 2006), *C. parasitica* populations in Ticino are considered as sexually reproducing. Therefore, we investigated mating type frequencies in both samplings. The mating types in the 1990s sampling were at a balanced ratio of 35 *MAT-1* isolates, 36 *MAT-2* isolates and three heterokaryons (i.e., with both mating type idiomorphs; Figure 5a). In contrast, the 2019 sampling was skewed towards *MAT-2*, with 42 *MAT-2* isolates (61.8%), 20 *MAT-1* isolates (29.4%) and six heterokaryons (8.8%). However, the overall shift in mating type ratios across sampling years (1990s vs. 2019) was not significant (Fisher's exact test; $p = .054$). When comparing changes in mating type ratios across the dominant *vc* types (EU-01, EU-02 and EU-05, Figure 5a), we detected a marginally significant increase in *MAT-2* for *vc* type

TABLE 3 Expected (under random mating) and observed *vc* type diversity in relation to the number of observed polymorphic *vic* loci in all *Cryphonectria parasitica* populations and at both samplings

	First sampling (1990s)			Second sampling (2019)			1990s vs. 2019 samplings		
Population	Polymorphic *vic* loci (*n*)	Observed *vc* types (*n*)	Potential *vc* types (*n*)	Polymorphic *vic* loci (*n*)	Observed *vc* types (*n*)	Potential *vc* types (*n*)	χ^2	*df*	*p*-value[a]
Lumino	5	9	32	5	8	32	13.1	12	.3621
Gnosca	5	7	32	4	5	16	7.7	7	.3567
Novaggio	4	6	16	5	8	32	12.2	9	.2037

[a]Differences in the number of observed *vc* types between samplings were considered significant at $p < .05$.

EU-02 (Fisher's exact test; $p = .03$). However, the increased incidence of *MAT-2* in the 2019 sampling appears not to be caused by clonal reproduction, as we found no increase in *MAT-2* clones (IBD = 1) in the 2019 sampling either for the EU-02 or for other *vc* types. Frequencies of *vc* types in the Ticino populations were relatively stable across both samplings, with EU-01, EU-02, EU-05 and EU-06 being the most abundant *vc* types (Figure 5a). Overall, the observed *vc* type diversity was lower than expected under random mating (Table 3). Differences in *vc* type diversity between samplings were not significant across samplings (Table 3). Furthermore, we found no associations between *vc* types and mating types.

3.6 | CHV1 prevalence and contributors to genome-wide diversity

Virus incidence appeared to be relatively stable over time, with 32.4% and 29.4% of *C. parasitica* isolates being infected in the 1990s and 2019 samplings, respectively. We additionally investigated the prevalence of CHV1 among the different *vc* types and mating types in both samplings. Virus incidence was higher in abundant *vc* types, but was also detected in some rare *vc* types (Figure 5b). Notably, in the 2019 sampling the majority of *MAT-2* isolates of *vc* type EU-01 were found to be virus-free (Figure 5b, 12 vs. one isolate). Although mating type ratios, *vc* type diversity and CHV1 prevalence varied among sampling sites, we did not observe spatial clustering of *vc* types and CHV1-infected isolates in 2019 (Figure 1). To test for the association of *vc* and mating types, presence/absence of CHV1-infection, as well as the sampling site with genetic diversity as inferred by IBS, we performed a PERMANOVA. The analysis revealed that only *vc* types significantly explained variation in the observed genetic diversity ($p < .001$, Table S6). The corresponding R^2 values and effect size suggest that the association with *vc* types increased over the sampling period ($R^2 = .82$ and .98 in the first and second sampling, respectively).

4 | DISCUSSION

We assessed temporal changes in population structure of the chestnut blight pathogen *Cryphonectria parasitica* and the prevalence of its hyperparasitic mycovirus CHV1 in Ticino (southern Switzerland) over three decades. Overall, we detected no substantial changes in the pathogen population structure over the study period, but populations showed signals of increased mating among related individuals. Only one out of five polymorphic *vic* loci observed in this study showed detectable signals of balancing selection, while allele frequencies at all other *vic* loci were highly imbalanced. Similarly, the number of observed *vc* types was lower than expected from the observed polymorphism at *vic* loci. This suggests that chestnut blight populations in southern Switzerland have not yet recovered from the recent migratory bottleneck triggered by the invasion of Europe. While overall low vegetative compatibility barriers facilitate the spread of CHV1, the observed CHV1 infection rate remained at ~30%. The combined results suggest the pathogen–hyperparasite interaction is cycling between expanding CHV1 infections and virus escape by the host, underpinning the observed retained stability.

4.1 | Retention of pathogen diversity facilitates mycovirus spread

The mycovirus CHV1 has been shown to have a significant negative impact on the fitness of its fungal host *C. parasitica*, in particular on parasitic growth and sporulation capacity (Brusini et al., 2017; Choi & Nuss, 1992). Hence, CHV1 may influence fungal population dynamics and act as a selective force at *vic* loci to limit virus transmission within the population. However, we found no evidence that CHV1 presence significantly affected genetic diversity of *C. parasitica* populations in southern Switzerland. Considering the parasitic nature of CHV1, *C. parasitica* populations are expected to attain a state of high *vc* type diversity to reduce virus transmission, as *vic* alleles have previously been found to be under balancing selection (Milgroom et al., 2018). In our study, balancing selection was only detected at one (i.e., *vic2*) of the six known *vic* loci. Both alleles at *vic2* show relatively strong virus inhibition effects (Cortesi et al., 2001). The highly skewed allele frequencies at the other *vic* loci may be an indication of weak or no balancing selection. Highly skewed allele frequencies at *vic* loci are expected to reduce the power of selection scans to detect signatures of balancing selection. Furthermore, sequence signatures of balancing selection are expected to arise over long evolutionary time periods rather than a few generations.

The diversity and prevalence of *vc* types in the studied populations did not change substantially over the span of three decades between samplings. Both in the 1990s and in 2019, Ticino populations were largely dominated by *vc* types EU-01, EU-02 and EU-05 (and partially EU-06), which are the most frequent *vc* types in central Europe (Robin & Heiniger, 2001). A relative stability of *vc* type diversity over time was also recently reported by Ježić et al. (2021) for other *C. parasitica* populations in Switzerland, Croatia and North Macedonia. These results of retained low *vc* type diversity in the presence of a deleterious mycovirus are in striking contrast to findings on the invasive forest pathogen *Ophiostoma novo-ulmi*, the causal agent of Dutch elm disease. While parasitic mycoviruses were at first highly abundant in clonal *O. novo-ulmi* populations, the acquisition of the opposite mating type and *vic* loci from a closely related sister species resulted in vast population diversification and rapid decline of mycovirus abundance (Brasier & Webber, 2019). Beside the capillary presence of CHV1, the absence of *vc* type diversification in the *C. parasitica* population in Ticino might be at least partially due to the invasion history of the pathogen. First, the introduction of *C. parasitica* into central–western Europe is recent (1930s–1950s) and *vic* alleles have not yet reached a state of equilibrium (Milgroom & Cortesi, 1999). Second, since the most dominant *vc* types (i.e., EU-01, EU-02, EU-05, EU-06) in central Europe exhibit fixed alleles at four *vic* loci (Figure S6; Cortesi & Milgroom, 1998), sexual recombination among these *vc* types does not result in the formation of new types. In the absence of substantial rates of clonality, low *vc* type diversity in *C. parasitica* populations is probably maintained by high rates of mating among related individuals of dominant *vc* types, selfing as well as genetic drift. This is in line with observations made in other invasive species that frequently undergo severe genetic bottlenecks upon introduction, resulting in reduced genetic diversity, inbreeding and genetic drift (Schrieber & Lachmuth, 2017).

4.2 | Mating among related fungal individuals

Cryphonectria parasitica populations in southern Switzerland show strong signatures of nonrandom mating. The presence of both mating types in all dominant *vc* types further points to high levels of mating among those *vc* types, as well as selfing, rather than clonal propagation. This results in a major contribution of *vic* loci to the overall observed genome-wide diversity. The high levels of mating among related individuals further support the hypothesis of the effects of a recent genetic bottleneck in the local *C. parasitica* population. Field experiments with the plant pathogen *Phytophthora capsici* showed that an experimentally induced bottleneck resulted in severe inbreeding within a few generations (Carlson et al., 2017). Strikingly, we found skewed mating type ratios in 2019, with an overrepresentation of mating type *MAT-2* at all sampled sites. In the absence of strong signals for clonal reproduction, this could indicate selfing or unisexual reproduction (i.e., sexual reproduction in the absence of the opposite mating type (Feretzaki & Heitman, 2013). Unisexual reproduction has been reported in several fungal species, including *Cryptococcus neoformans*, *Neurospora* spp. and *Huntiella moniliformis* (Glass & Smith, 1994; Lin et al., 2005; Sun et al., 2014; Wilson et al., 2015). In *C. parasitica*, McGuire et al. (2004) reported no mating type segregation among progeny from perithecia that resulted from selfing. The molecular mechanisms and factors triggering such events in *C. parasitica* remain poorly resolved. However, unisexual reproduction might constitute a plausible mechanism to explain skewed mating type ratios in sexually reproducing *C. parasitica* populations.

4.3 | CHV1 infection dynamics in *C. parasitica* populations

Our study shows stable CHV1 infection rates of ~30% among bark cankers over a period of ~30 years in *C. parasitica* populations in Ticino. This CHV1 incidence is below the previously reported range of 40%–75% for populations in the same region (Bissegger et al., 1997; Bryner et al., 2012; Ježić et al., 2021). The difference may be due to the fact that most cankers sampled in 2019 were inactive (i.e., no fungal growth resulting in canker extension). Such cankers, although not lethal for the infected trees, are frequently CHV1-free (Bryner et al., 2014; Ježić et al., 2019). CHV1 drastically slows down the metabolism of its fungal host, resulting in the inactivation of chestnut blight cankers. Paradoxically, this may negatively affect survival of CHV1 itself, which might eventually disappear from the inactivated cankers (Bryner et al., 2014). As a consequence, highly deleterious CHV1 strains might be less likely to persist and spread within a fungal population due to the strong negative fitness impact they assert on their fungal host (Morozov et al., 2007). Previous studies in which the same cankers were repeatedly sampled over a few years revealed a highly dynamic system, in which cankers may change between virus-infected and virus-free states (Bryner et al., 2014; Ježić et al., 2018). Virus infection dynamics in *C. parasitica* populations could further be influenced by the chestnut blight canker microbiome. Recent findings on the American chestnut (*Castanea dentata*) suggest that CHV1 persistence might be influenced by other fungi residing in the cankers, potentially promoting the resurgence of virulent *C. parasitica* by outcompeting hypovirulent *C. parasitica* strains (Kolp et al., 2020). Although our results suggest long-term stability of CHV1 infection in *C. parasitica* populations with naturally occurring hypovirulence, the underlying fungal–viral dynamics may not be captured well by overall infection rates. Interestingly, Leigh et al. (2021) recently showed higher CHV1 intrahost diversity in older chestnut blight cankers due to accumulation of predominantly synonymous mutations. However, further studies are required to elucidate the temporal persistence and virulence of individual viral genotypes in *C. parasitica* populations.

4.4 | Role of the host tree in the pathogen–hyperparasite interaction

Although non-native to the study area, *Castanea sativa* was introduced into southern Switzerland as early as during the Roman period (Conedera et al., 2004) and the species is currently considered to be naturalized. A study based on microsatellite markers revealed a high genetic diversity of local chestnut populations (Beccaro et al., 2012), which seem connected to a main European gene pool (Mattioni et al., 2008). Nonetheless, there is no evidence for resistance in *Castanea sativa* (Bryner et al., 2012) and CHV1 remains the most effective biological control agent against chestnut blight in Europe. While the long generation times of the tree host potentially translate into slower adaptation, standing genetic variation could mitigate pathogen damage through perennial buffering of boom and bust cycles or phenological mismatching (Brown & Tellier, 2011; Budde et al., 2016; Tellier & Brown, 2009) . In oaks, later physiological activity in spring has been associated with reduced infection rates with *Phytophthora ramorum* (Dodd et al., 2008). In *Castanea sativa*, seasonal patterns in the development of bark cankers caused by *C. parasitica* were observed by Guérin and Robin (2003). Such differences resulted from seasonal variation in chestnut susceptibility and the effect of climatic factors on the pathogen (Guérin & Robin, 2003). In southern Switzerland, most chestnut trees regrow as vegetative sprouts from existing stumps or dead trees. Therefore, changes over time in host genetic diversity are probably minimal and genetic resistance against chestnut blight is unlikely to evolve quickly. Thanks to the widespread presence of hypovirulence in Europe and the current effectiveness of CHV1 as a biocontrol agent for chestnut blight, the development of resistance toward *C. parasitica* might not even be a *sine qua non* condition for the survival of *Castanea sativa*. However, the interaction *C. parasitica* – CHV1 on *Castanea sativa* is evolutionarily new and the resulting hypovirulence could be altered following changes in the pathogen (e.g., introduction or emergence of new *vc* types), the hyperparasite (e.g., loss of virulence) or the environment.

ACKNOWLEDGEMENTS

We thank Eva Augustiny, Silvia Kobel, Aria Minder, Quirin Kupper and Hélène Blauenstein for help in sampling and laboratory assistance. We acknowledge the Genetic Diversity Centre (GDC), ETH Zurich, and the Functional Genomics Center Zurich (FGCZ) for technical support and facility access. Franziska Schmid greatly helped with spatial visualizations. Thanks to Alice Feurtey and Pierre Gladieux for insightful discussions, Danilo Pereira and Thomas Badet for sharing scripts, and Daniel Rigling for critically reading the manuscript. We thank the three anonymous reviewers for their valuable comments on a previous version of the manuscript. L.S. was supported by the Swiss National Science Foundation (grant 170188 to S.P.). Open Access Funding provided by Lib4RI Library for the Research Institutes within the ETH Domain Eawag Empa PSI and WSL.

AUTHOR CONTRIBUTIONS

L.S. performed research, analysed data and wrote the original draft. D.C. designed the study, supervised data analysis and edited the paper. S.P. designed the study, acquired funds and edited the paper.

CONFLICT OF INTEREST

The authors declare no conflict of interest.

DATA AVAILABILITY STATEMENT

All raw read sequences are available at the NCBI Sequence Read Archive (SRA) Bioprojects PRJNA604575, PRJNA644891 and PRJNA644891. Data sets and scripts for all analyses are accessible at: https://github.com/Cryphonectria/Stauber2022_MolEcol.

ORCID

Lea Stauber https://orcid.org/0000-0001-8367-6150
Daniel Croll https://orcid.org/0000-0002-2072-380X
Simone Prospero https://orcid.org/0000-0002-9129-8556

REFERENCES

Alachiotis, N., & Pavlidis, P. (2018). RAiSD detects positive selection based on multiple signatures of a selective sweep and SNP vectors. *Communications Biology*, *1*(1), 1–11. https://doi.org/10.1038/s42003-018-0085-8

Anagnostakis, S. L. (1982). Biological control of chestnut blight. *Science*, *215*(4532), 466–471.

Anagnostakis, S. L. (1988). *Cryphonectria parasitica*, Cause of Chestnut Blight. In: *Advances in Plant Pathology* (Vol. *6*)123–136. Academic Press Limited. https://doi.org/10.1016/B978-0-12-033706-4.50011-6

Anderson, M. J. (2001). A new method for non-parametric multivariate analysis of variance. *Austral Ecology*, *26*(1), 32–46. https://doi.org/10.1046/j.1442-9993.2001.01070.x

Barrett, L. G., Thrall, P. H., Burdon, J. J., & Linde, C. C. (2008). Life history determines genetic structure and evolutionary potential of host–parasite interactions. *Trends in Ecology & Evolution*, *23*(12), 678–685. https://doi.org/10.1016/j.tree.2008.06.017

Beccaro, G. L., Torello-Marinoni, D., Binelli, G., Donnon, D., Boccacci, P., Botta, R., Cerutti, A. K., & Conedera, M. (2012). Insights in the chestnut genetic diversity in Canton Ticino (Southern Switzerland). *Silvae Genetica*, *61*, 292–300. https://doi.org/10.1515/sg-2012-0037

Belov, A. A., Witte, T. E., Overy, D. P., & Smith, M. L. (2021). Transcriptome analysis implicates secondary metabolite production, redox reactions, and programmed cell death during allorecognition in *Cryphonectria parasitica*. *G3*, *11*(1), 1–13.

Bissegger, M., Rigling, D., & Heiniger, U. (1997). Population structure and disease development of *Cryphonectria parasitica* in European chestnut forests in the presence of natural hypovirulence. *Phytopathology*, *87*(1), 50–59. https://doi.org/10.1094/PHYTO.1997.87.1.50

Bougeard, S., & Dray, S. (2018). Supervised multiblock analysis in R with the ade4 package. *Journal of Statistical Software*, *86*(1), 1–17.

Bradbury, P. J., Zhang, Z., Kroon, D. E., Casstevens, T. M., Ramdoss, Y., & Buckler, E. S. (2007). TASSEL: software for association mapping of complex traits in diverse samples. *Bioinformatics*, *23*(19), 2633–2635. https://doi.org/10.1093/bioinformatics/btm308

Branine, M., Bazzicalupo, A., & Branco, S. (2019). Biology and applications of endophytic insect-pathogenic fungi. *PLoS Path*, *15*(7), e1007831. https://doi.org/10.1371/journal.ppat.1007831

Brasier, C. M., & Webber, J. F. (2019). Is there evidence for post-epidemic attenuation in the Dutch elm disease pathogen *Ophiostoma novo-ulmi*? *Plant Pathology*, *68*(5), 921–929.

Brown, J. K. M., & Tellier, A. (2011). Plant-parasite coevolution: bridging the gap between genetics and ecology. *Annual Review of Phytopathology*, *49*, 345–367. https://doi.org/10.1146/annurev-phyto-072910-095301

Brusini, J., Wayne, M. L., Franc, A., & Robin, C. (2017). The impact of parasitism on resource allocation in a fungal host: the case of *Cryphonectria parasitica* and its mycovirus, Cryphonectria Hypovirus 1. *Ecology and Evolution*, *7*(15), 5967–5976.

Bryner, S. F., Prospero, S., & Rigling, D. (2014). Dynamics of *Cryphonectria hypovirus* infection in chestnut blight cankers. *Phytopathology*, *104*(9), 918–925.

Bryner, S. F., Rigling, D., & Brunner, P. C. (2012). Invasion history and demographic pattern of *Cryphonectria hypovirus 1* across European populations of the chestnut blight fungus. *Ecology and Evolution*, *2*(12), 3227–3241.

Budde, K. B., Nielsen, L. R., Ravn, H. P., & Kjær, E. D. (2016). The natural evolutionary potential of tree populations to cope with newly introduced pests and pathogens-lessons learned from forest health catastrophes in recent decades. *Current Forestry Reports*, *2*, 18–29. https://doi.org/10.1007/s40725-016-0029-9

Carlson, M. O., Gazave, E., Gore, M. A., & Smart, C. D. (2017). Temporal genetic dynamics of an experimental, biparental field population of *Phytophthora capsici*. *Frontiers in Genetics*, *8*, 1–19. https://doi.org/10.3389/fgene.2017.00026

Choi, G. H., & Nuss, D. L. (1992). Hypovirulence of chestnut blight fungus conferred by an infectious viral cDNA. *Science*, *257*(5071), 800–803.

Chun, J., Ko, Y.-H., & Kim, D.-H. (2020). Transcriptome analysis of *Cryphonectria parasitica* infected with Cryphonectria hypovirus 1 (CHV1) reveals distinct genes related to fungal metabolites, virulence, antiviral RNA-silencing, and their regulation. *Frontiers in Microbiology*, *11*, 1711. https://doi.org/10.3389/fmicb.2020.01711

Cingolani, P., Platts, A., Wang, L. L., Coon, M., Nguyen, T., Wang, L., Land, S. J., Lu, X., & Ruden, D. M. (2012). A program for annotating and predicting the effects of single nucleotide polymorphisms, SnpEff: SNPs in the genome of *Drosophila melanogaster* strain w1118; iso-2; iso-3. *Fly*, *6*(2), 80–92. https://doi.org/10.4161/fly.19695

Conedera, M., Krebs, P., Tinner, W., Pradella, M., & Torriani, D. (2004). The cultivation of *Castanea sativa* (Mill.) in Europe, from its origin to its diffusion on a continental scale. *Vegetation History and Archaeobotany*, *13*, 161–179.

Cornejo, C., Šever, B., Kupper, Q., Prospero, S., & Rigling, D. (2019). A multiplexed genotyping assay to determine vegetative incompatibility and mating type in *Cryphonectria parasitica*. *European Journal of Plant Pathology*, *155*(1), 81–91.

Cortesi, P., McCulloch, C. E., Song, H., Lin, H., & Milgroom, M. G. (2001). Genetic control of horizontal virus transmission in the chestnut blight fungus, Cryphonectria Parasitica. *Genetics*, *159*(1), 107–118.

Cortesi, P., & Milgroom, M. G. (1998). Genetics of vegetative incompatibility in *Cryphonectria parasitica*. *Applied and Environmental Microbiology*, *64*(8), 2988–2994. https://doi.org/10.1128/aem.64.8.2988-2994.1998

Crouch, J. A., Dawe, A., Aerts, A., Barry, K., Churchill, A. C. L., Grimwood, J., Hillman, B. I., Milgroom, M. G., Pangilinan, J., Smith, M., Salamov, A., Schmutz, J., Yadav, J. S., Grigoriev, I. V., & Nuss, D. L. (2020). Genome sequence of the chestnut blight fungus *Cryphonectria parasitica* EP155: A fundamental resource for an archetypical invasive plant pathogen. *Phytopathology*, *110*(6), 1180–1188.

Danecek, P., Auton, A., Abecasis, G., Albers, C. A., Banks, E., DePristo, M. A., Handsaker, R. E., Lunter, G., Marth, G. T., Sherry, S. T., McVean, G., & Durbin, R. (2011). The variant call format and VCFtools. *Bioinformatics*, *27*(15), 2156–2158. https://doi.org/10.1093/bioinformatics/btr330

Demené, A., Legrand, L., Gouzy, J., Debuchy, R., Saint-Jean, G., Fabreguettes, O., & Dutech, C. (2019). Whole-genome sequencing reveals recent and frequent genetic recombination between clonal lineages of *Cryphonectria parasitica* in western Europe. *Fungal Genetics and Biology*, *130*, 122–133. https://doi.org/10.1016/j.fgb.2019.06.002

Diamandis, S., Perlerou, C., Nakopoulou, Z., Christopoulos, E., Topalidou, E., & Tziros, G. (2014). Application of biological control of chestnut blight on a nationwide scale in Greece: Results and prospects. *Acta Horticulturae*, *1043*, 23–34.

Dodd, R. S., Hüberli, D., Mayer, W., Harnik, T. Y., Afzal-Rafii, Z., & Garbelotto, M. (2008). Evidence for the role of synchronicity between host phenology and pathogen activity in the distribution of sudden oak death canker disease. *New Phytologist*, *179*(2), 505–514. https://doi.org/10.1111/j.1469-8137.2008.02450.x

Dumartinet, T., Abadie, C., Bonnot, F., Carreel, F., Roussel, V., Habas, R., Martinez, R. T., Perez-Vicente, L., & Carlier, J. (2020). Pattern of local adaptation to quantitative host resistance in a major pathogen of a perennial crop. *Evolutionary Applications*, *13*(4), 824–836. https://doi.org/10.1111/eva.12904

Dutech, C., Barrès, B., Bridier, J., Robin, C., Milgroom, M. G., & Ravigné, V. (2012). The chestnut blight fungus world tour: Successive introduction events from diverse origins in an invasive plant fungal pathogen. *Molecular Ecology*, *21*(16), 3931–3946. https://doi.org/10.1111/j.1365-294X.2012.05575.x

Elliston, J. E. (1982). Hypovirulence. *Advances in Plant Pathology*, *1*, 1–33.

Feretzaki, M., & Heitman, J. (2013). Unisexual reproduction drives evolution of eukaryotic microbial pathogens. *PLoS Path*, *9*(10), e1003674. https://doi.org/10.1371/journal.ppat.1003674

Ford, S. A., Williams, D., Paterson, S., & King, K. C. (2017). Co-evolutionary dynamics between a defensive microbe and a pathogen driven by fluctuating selection. *Molecular Ecology*, *26*(7), 1778–1789. https://doi.org/10.1111/mec.13906

Glass, N. L., & Kaneko, I. (2003). Fatal attraction: Nonself recognition and heterokaryon incompatibility in filamentous fungi. *Eukaryotic Cell*, *2*(1), 1–8. https://doi.org/10.1128/EC.2.1.1-8.2003

Glass, N. L., & Smith, M. L. (1994). Structure and function of a mating-type gene from the homothallic species *Neurospora africana*. *Molecular and General Genetics*, *244*(4), 401–409. https://doi.org/10.1007/BF00286692

Gobbin, D., Hoegger, P. J., Heiniger, U., & Rigling, D. (2003). Sequence variation and evolution of Cryphonectria hypovirus 1 (CHV-1) in Europe. *Virus Research*, *97*(1), 39–46. https://doi.org/10.1016/S0168-1702(03)00220-X

Grente, M. J. (1965). Les formes hypovirulentes d'*Endothia parasitica* et les espoirs de lutte contre le chancre du châtaignier. *Académie D'agriculture De France*, *51*, 1033–1036.

Guérin, L., & Robin, C. (2003). Seasonal effect on infection and development of lesions caused by *Cryphonectria parasitica* in *Castanea sativa*. *Forest Pathology*, *33*(4), 223–235. https://doi.org/10.1046/j.1439-0329.2003.00329.x

Heiniger, U., & Rigling, D. (1994). Biological control of chestnut blight in Europe. *Annual Review of Phytopathology*, *32*(1), 581–599. https://doi.org/10.1146/annurev.py.32.090194.003053

Heiniger, U., & Rigling, D. (2009). Application of the *Cryphonectria Hypovirus* (CHV-1) to control the chestnut blight, experience from Switzerland. *Acta Horticulturae*, *815*, 233–245.

Hessenauer, P., Feau, N., Gill, U., Schwessinger, B., Brar, G. S., & Hamelin, R. C. (2021). Evolution and adaptation of forest and crop pathogens in the Anthropocene. *Phytopathology*, *111*(1), 49–67. https://doi.org/10.1094/phyto-08-20-0358-fi

Hudson, R. R. (2002). Generating samples under a Wright-Fisher neutral model of genetic variation. *Bioinformatics*, *18*(2), 337–338. https://doi.org/10.1093/bioinformatics/18.2.337

Huson, D. H., Kloepper, T., & Bryant, D. (2008). SplitsTree 4.0-Computation of phylogenetic trees and networks. *Bioinformatics*, *14*, 68–73.

Ježić, M., Kolp, M., Prospero, S., Karin-Kujundžić, V., Idžojtić, M., Sotirovski, K., Risteski, M., Rigling, D., Double, M. L., & Ćurković-Perica, M. (2019). Diversity of *Cryphonectria parasitica* in callused chestnut blight cankers on European and American chestnut. *Forest Pathology*, *49*, e12566.

Ježić, M., Mlinarec, J., Vuković, R., Katanić, Z., Krstin, L., Nuskern, L., Poljak, I., Idžojtić, M., Tkalec, M., & Ćurković-Perica, M. (2018). Changes in *Cryphonectria parasitica* populations affect natural biological control of chestnut blight. *Phytopathology*, *108*(7), 870–877. https://doi.org/10.1094/PHYTO-07-17-0252-R

Ježić, M., Schwarz, J. M., Prospero, S., Sotirovski, K., Risteski, M., Ćurković-Perica, M., Nuskern, L., Krstin, L., Katanić, Z., Dejanović, E., Poljak, I., Idžojtić, M., & Rigling, D. (2021). Temporal and spatial genetic population structure of *Cryphonectria parasitica* and its associated hypovirus across an invasive range of chestnut blight in Europe. *Phytopathology*, *111*(8), 1327–1337. https://doi.org/10.1094/PHYTO-09-20-0405-R

Jombart, T. (2008). adegenet: A R package for the multivariate analysis of genetic markers. *Bioinformatics*, *24*(11), 1403–1405. https://doi.org/10.1093/bioinformatics/btn129

Jombart, T., Devillard, S., & Balloux, F. (2010). Discriminant analysis of principal components: A new method for the analysis of genetically structured populations. *BMC Genetics*, *11*(1), 1–15.

Jones, P., Binns, D., Chang, H.-Y., Fraser, M., Li, W., McAnulla, C., McWilliam, H., Maslen, J., Mitchell, A., Nuka, G., Pesseat, S., Quinn, A. F., Sangrador-Vegas, A., Scheremetjew, M., Yong, S.-Y., Lopez, R., & Hunter, S. (2014). InterProScan 5: Genome-scale protein function classification. *Bioinformatics*, *30*(9), 1236–1240. https://doi.org/10.1093/bioinformatics/btu031

Kamvar, Z. N., Tabima, J. F., & Grünwald, N. J. (2014). Poppr: An R package for genetic analysis of populations with clonal, partially clonal, and/or sexual reproduction. *PeerJ*, *2*, e281.

Kolp, M., Double, M. L., Fulbright, D. W., MacDonald, W. L., & Jarosz, A. M. (2020). Spatial and temporal dynamics of the fungal community of chestnut blight cankers on American chestnut (*Castanea dentata*) in Michigan and Wisconsin. *Fungal Ecology*, *45*, 100925. https://doi.org/10.1016/j.funeco.2020.100925

Koskella, B. (2013). Phage-mediated selection on microbiota of a long-lived host. *Current Biology*, *23*(13), 1256–1260. https://doi.org/10.1016/j.cub.2013.05.038

Krstin, L., Novak-Agbaba, S., Rigling, D., & Ćurković-Perica, M. (2011). Diversity of vegetative compatibility types and mating types of *Cryphonectria parasitica* in Slovenia and occurrence of associated *Cryphonectria hypovirus 1*. *Plant Pathology*, *60*(4), 752–761. https://doi.org/10.1111/j.1365-3059.2011.02438.x

Leigh, D. M., Peranić, K., Prospero, S., Cornejo, C., Ćurković-Perica, M., Kupper, Q., Nuskern, L., Rigling, D., & Ježić, M. (2021). Long-read sequencing reveals the evolutionary drivers of intra-host diversity across natural RNA mycovirus infections. *Virus Evolution*, *7*(2), veab101. https://doi.org/10.1093/ve/veab101

Lin, X., Hull, C. M., & Heitman, J. (2005). Sexual reproduction between partners of the same mating type in *Cryptococcus neoformans*. *Nature*, *434*(7036), 1017–1021.

Mattioni, C., Cherubini, M., Micheli, E., Villani, F., & Bucci, G. (2008). Role of domestication in shaping *Castanea sativa* genetic variation in Europe. *Tree Genetics & Genomes*, *4*, 563–574. https://doi.org/10.1007/s11295-008-0132-6

McGuire, I. C., Marra, R. E., & Milgroom, M. G. (2004). Mating-type heterokaryosis and selfing in *Cryphonectria parasitica*. *Fungal Genetics and Biology*, *41*(5), 521–533. https://doi.org/10.1016/j.fgb.2003.12.007

McGuire, I. C., Marra, R. E., Turgeon, B. G., & Milgroom, M. G. (2001). Analysis of mating-type genes in the chestnut blight fungus, Cryphonectria Parasitica. *Fungal Genetics and Biology*, *34*(2), 131–144. https://doi.org/10.1006/fgbi.2001.1295

McVean, G., & Auton, A. (2007). LDhat 2.1: A package for the population genetic analysis of recombination. *Department of Statistics, Oxford, OX1 3TG, UK*.

Mei, L., Chen, M., Shang, Y., Tang, G., Tao, Y., Zeng, L., Huang, B., Li, Z., Zhan, S., & Wang, C. (2020). Population genomics and evolution of a fungal pathogen after releasing exotic strains to control insect pests for 20 years. *The ISME Journal*, *14*(6), 1422–1434. https://doi.org/10.1038/s41396-020-0620-8

Milgroom, M. G., & Cortesi, P. (1999). Analysis of population structure of the chestnut blight fungus based on vegetative incompatibility genotypes. *Proceedings of the National Academy of Sciences of the United States of America*, *96*(18), 10518–10523. https://doi.org/10.1073/pnas.96.18.10518

Milgroom, M. G., Smith, M. L., Drott, M. T., & Nuss, D. L. (2018). Balancing selection at nonself recognition loci in the chestnut blight fungus, *Cryphonectria parasitica*, demonstrated by trans-species polymorphisms, positive selection, and even allele frequencies. *Heredity*, *121*(6), 511–523. https://doi.org/10.1038/s41437-018-0060-7

Milgroom, M. G., Wang, K., Zhou, Y., Lipari, S. E., & Kaneko, S. (1996). Intercontinental population structure of the chestnut blight fungus, Cryphonectria Parasitica. *Mycologia*, *88*(2), 179–190. https://doi.org/10.2307/3760921

Morozov, A. Y., Robin, C., & Franc, A. (2007). A simple model for the dynamics of a host-parasite-hyperparasite interaction. *Journal of Theoretical Biology*, *249*(2), 246–253. https://doi.org/10.1016/j.jtbi.2007.05.041

Nuss, D. L. (2005). Hypovirulence: Mycoviruses at the fungal-plant interface. *Nature Reviews Microbiology*, *3*(8), 632–642. https://doi.org/10.1038/nrmicro1206

Oksanen, J., Blanchet, F. G., Friendly, M., Kindt, R., Legendre, P., McGlinn, D., & Wagner, H. (2019). *vegan: Community Ecology Package*. Retrieved from https://cran.r-project.org/package=vegan

Parratt, S. R., & Laine, A. L. (2016). The role of hyperparasitism in microbial pathogen ecology and evolution. *The ISME Journal*, *10*(8), 1815–1822. https://doi.org/10.1038/ismej.2015.247

Prospero, S., Conedera, M., Heiniger, U., & Rigling, D. (2006). Saprophytic activity and sporulation of *Cryphonectria parasitica* on dead chestnut wood in forests with naturally established hypovirulence. *Phytopathology*, *96*(12), 1337–1344.

Prospero, S., & Rigling, D. (2012). Invasion genetics of the chestnut blight fungus *Cryphonectria parasitica* in Switzerland. *Phytopathology*, *102*(1), 73–82. https://doi.org/10.1094/PHYTO-02-11-0055

Reyes, A., Wu, M., McNulty, N. P., Rohwer, F. L., & Gordon, J. I. (2013). Gnotobiotic mouse model of phage–bacterial host dynamics in the human gut. *Proceedings of the National Academy of Sciences*, *110*(50), 20236–20241. https://doi.org/10.1073/pnas.1319470110

Rigling, D., & Prospero, S. (2018). *Cryphonectria parasitica*, the causal agent of chestnut blight: Invasion history, population biology and disease control. *Molecular Plant Pathology*, *19*(1), 7–20. https://doi.org/10.1111/mpp.12542

Robin, C., & Heiniger, U. (2001). Chestnut blight in Europe: diversity of *Cryphonectria parasitica*, hypovirulence and biocontrol. *Forest Snow and Landscape Research*, *76*, 361–367.

Schaffner, S. F., Taylor, A. R., Wong, W., Wirth, D. F., & Neafsey, D. E. (2018). hmmIBD: Software to infer pairwise identity by descent between haploid genotypes. *Malaria Journal*, *17*(1), 196. https://doi.org/10.1186/s12936-018-2349-7

Schrieber, K., & Lachmuth, S. (2017). The genetic paradox of invasions revisited: The potential role of inbreeding × environment interactions in invasion success. *Biological Reviews*, *92*(2), 939–952. https://doi.org/10.1111/brv.12263

Siewert, K. M., & Voight, B. F. (2017). Detecting long-term balancing selection using allele frequency correlation. *Molecular Biology and Evolution*, *34*(11), 2996–3005. https://doi.org/10.1093/molbev/msx209

Sotirovski, K., Papazova-Anakieva, I., Grünwald, N. J., & Milgroom, M. G. (2004). Low diversity of vegetative compatibility types and mating type of *Cryphonectria parasitica* in the southern Balkans. *Plant Pathology*, *53*(3), 325–333. https://doi.org/10.1111/j.0032-0862.2004.01006.x

Stauber, L., Badet, T., Feurtey, A., Prospero, S., & Croll, D. (2021). Emergence and diversification of a highly invasive chestnut pathogen lineage across south-eastern Europe. *Elife*, *10*, e56279. https://doi.org/10.1101/2020.02.15.950170

Stauber, L., Prospero, S., & Croll, D. (2020). Comparative genomics analyses of lifestyle transitions at the origin of an invasive fungal pathogen in the genus *Cryphonectria*. *Msphere*, *5*(5), 1–17. https://doi.org/10.1128/msphere.00737-20

Sun, S., Billmyre, R. B., Mieczkowski, P. A., & Heitman, J. (2014). Unisexual reproduction drives meiotic recombination and phenotypic and karyotypic plasticity in *Cryptococcus neoformans*. *PLoS Genetics*, *10*(12), e1004849. https://doi.org/10.1371/journal.pgen.1004849

Tellier, A., & Brown, J. K. M. (2009). The influence of perenniality and seed banks on polymorphism in plant-parasite interactions. *The American Naturalist*, *174*(6), 769–779. https://doi.org/10.1086/646603

Tian, B., Yang, J., & Zhang, K.-Q. (2007). Bacteria used in the biological control of plant-parasitic nematodes: populations, mechanisms of action, and future prospects. *FEMS Microbiology Ecology*, *61*(2), 197–213. https://doi.org/10.1111/j.1574-6941.2007.00349.x

Urayama, S., Katoh, Y., Fukuhara, T., Arie, T., Moriyama, H., & Teraoka, T. (2015). Rapid detection of Magnaporthe oryzae chrysovirus 1-A from fungal colonies on agar plates and lesions of rice blast. *Journal of General Plant Pathology*, *81*(2), 97–102. https://doi.org/10.1007/s10327-014-0567-6

Van Alfen, N. K. (1982). Biology and potential for disease control of hypovirulence of *Endothia parasitica*. *Annual Review of Phytopathology*, *20*, 349–362. https://doi.org/10.1146/annurev.py.20.090182.002025

Wilson, A. M., Godlonton, T., der Nest, M. A., Wilken, P. M., Wingfield, M. J., & Wingfield, B. D. (2015). Unisexual reproduction in *Huntiella moniliformis*. *Fungal Genetics and Biology*, *80*, 1–9. https://doi.org/10.1016/j.fgb.2015.04.008

Zhang, D.-X., Spiering, M. J., Dawe, A. L., & Nuss, D. L. (2014). Vegetative incompatibility loci with dedicated roles in allorecognition restrict mycovirus transmission in chestnut blight fungus. *Genetics*, *197*(2), 701–714. https://doi.org/10.1534/genetics.114.164574

Zheng, X., Levine, D., Shen, J., Gogarten, S., Laurie, C., & Weir, B. (2012). A high-performance computing toolset for relatedness and principal component analysis of SNP data. *Bioinformatics*, *28*(24), 3326–3328. https://doi.org/10.1093/bioinformatics/bts606

SUPPORTING INFORMATION

Additional supporting information may be found in the online version of the article at the publisher's website.

How to cite this article: Stauber, L., Croll, D., & Prospero, S. (2022). Temporal changes in pathogen diversity in a perennial plant–pathogen–hyperparasite system. *Molecular Ecology*, 31, 2073–2088. https://doi.org/10.1111/mec.16386